Mon. Not. R. Astron. Soc. **000**, 000–000 (0000) Printed 1 February 2008 (MN LATEX style file v1.4)

Imprints of Primordial Voids on the CMB

C. Baccigalupi[1,2], L. Amendola[1] and F. Occhionero[1]
[1] *Osservatorio Astronomico di Roma, Viale del Parco Mellini 84, 00136 Roma, Italy*
[2] *Department of Physics, University of Ferrara, Via del Paradiso 12, 44100 Ferrara, Italy*

1 February 2008

ABSTRACT
We generalize in several ways the results existing in the literature: a) we make use of an exact general relativistic solution for a spherical, nearly empty cavity in the matter dominated era to evaluate the null geodesics and the Sachs-Wolfe effect; b) we evaluate the magnitude of the adiabatic fluctuations of the photon-baryon plasma; c) we study the influence of the shell profile; and d) we take into account the finite thickness of the last scattering surface (LSS) and the influence of its position with respect to the void center. We find empirically an analytic approximation to the Sachs-Wolfe effect for all crossing geometries and we derive an upper limit of $\approx 25\ h^{-1}$ Mpc for the comoving radii of voids sitting on the LSS in order to achieve compatibility with COBE's data. As a nearly empty void has an overcomoving expansion of a factor of ≈ 4 between decoupling and the present, the maximum allowed size at present is $\approx 100\ h^{-1}$ Mpc. On the other hand, the smallness of the comoving size relative to the sound horizon reduces strongly the adiabatic effect by Silk damping and makes it negligible. Most of the signature of primordial voids comes therefore from metric effects and consists of subdegree spots blue or red depending on whether the center lies beyond or within the LSS. In conclusion we refine and confirm earlier constraints on a power law void spectrum originated in an inflationary phase transition and capable of generating the observed large scale structure.

1 INTRODUCTION

Inflation provides two well known mechanisms for relating primordial physics to perturbations on large scales ($\geq 10\ h^{-1}$Mpc) in the observed universe. The first one arises from the small quantum fluctuations of the inflaton field: the fluctuations are stretched out to scales greater than the horizon (H^{-1}) by the spatial expansion, and their dynamics freezes until the reenter in post-inflationary epochs. The second mechanism occurs in the case of a first order phase transition in the early universe; the nucleated bubbles imprint the density field. In fact, in this work we assume that they are the primordial cause of the large scale voids observed at the present. A class of inflationary models provides bubbles production; the underlying minimal physics is given by quantum field theory through quantum transition of the inflaton field from a false vacuum state to a true vacuum one. More realistic models of first order inflation (FOI), after the original version by Guth (1981), were found by considering non-minimal gravity theories and two-field phenomenology (see e.g. La & Steinhardt 1989, Kolb 1991, Adams & Freese 1991, Occhionero & Amendola 1994), and made FOI the richest extension of the slow-rolling model worked out by Linde (1983).

The hypothesis of a bubbly distribution of matter in the universe, theoretically interesting in itself, is strongly suggested by recent observations. Large-scale voids ($\geq 10\ h^{-1}$Mpc) have been discovered by recent redshift surveys (see e.g. Kauffmann & Fairall 1991, Vogeley, Geller & Huchra 1991, Lindner et al. 1995, and references therein), but the definition of a statistics for their dimensions is still premature, due to the presence of voids comparable with the sample's size. Deep ($1000\ h^{-1}$Mpc) pencil-beam surveys toward the galac-

tic poles revealed a fascinating regularity in the galaxy distribution with a characteristic scale of 128 h^{-1}Mpc (Broadhurst et al. 1990); El-Ad et al. (1996) constructed an algorithm to find voids in redshift surveys; da Costa et al. (1996) found that the voids are really empty of matter.

The estimate of the anisotropies induced by a void in the cosmic microwave background (CMB) yields the strongest constraint to the underlying inflationary physics by comparison with COBE observations (see e.g. Bennet et al. 1994 and references therein). Detections of degree scale CMB anisotropies (see e.g. Scott et al. 1996) provide in our case weaker constraints because they involve a limited part of the sky. To be quantitative, upgrading the experiment from 10 to 1 degree would imply a gain of a factor 100 in resolution; but in our case we would be looking for one single object, the largest, and we have to take into account the portion of sky in which we search (precisely rescaling by the corrisponding factor dN_B in Eq.(37) below). Consequently, such observations would be significative in our case if the covered solid angle were at least 400 square degrees, and to our knowledge high resolution observations of this width do not exist.

The first attempt to relate the evidence of voids in the large scale matter distribution with FOI was made by La in 1991. Overcoming the difficulties of previous works (Turner et al. 1992, Liddle & Wands 1991, 1992), it has been found that it is possible to construct models that fit the galaxy correlation function and pass the CMB bounds with a bubbly matter distribution (Amendola & Occhionero 1993, Amendola & Borgani 1994). Occhionero & Amendola (1994) found a toy model of FOI where the expected distribution in radius of the primordial voids, defined as the number of voids with radius greater than R today, is approximated by a power law,

$$N_B(R) = \left(\frac{R_M}{R}\right)^p \quad . \tag{1}$$

This distribution is compatible with the measured galaxy power spectrum and with the CMB anisotropies for

$$R_M \simeq 30 \ h^{-1}\mathrm{Mpc} \quad , \quad 6 < \mathrm{p} < 10 \quad , \tag{2}$$

normalizing N_B to a cube with 500 h^{-1}Mpc by side. Aim of this paper is to review and to set the constraint on R_M and p more rigorously than in the original paper, by an accurate evaluation of the physics involved.

A void is characterized by its central to asymptotical density ratio

$$\Delta = \frac{\rho_{center}}{\rho_\infty} \tag{3}$$

that decreases with time. The dynamics of voids has been investigated by Icke (1984) and Bertschinger (1983, 1985) in the strongly non-linear regime, $\Delta \ll 1$, and for $t \to \infty$. The important result of their analysis is that the physical radius r of a compensated void of total energy E increases as $t^{4/5}$ and that all the significative quantities of a void (pressure, density profile, velocity field, mass) are only functions of the dimensionless coordinate $\lambda = r(Et^2/\rho_\infty)^{-1/5}$, thus remaining unchanged at late times (self-similar expansion). These analyses have been confirmed by N-body simulations (White & Ostriker 1990, Dubinski et al. 1993). In the following we mean that R in Eq. (1) is the physical radius today; however, the corrisponding comoving quantity was smaller in the past by a factor of $(t/t_0)^{\frac{4}{5}-\frac{2}{3}} = (1+z)^{-0.2}$; in particular, a void on the last scattering surface (LSS), at $1 + z \simeq 1000$, was physically smaller by a factor of 4×1000.

If we connect present voids with primordial bubbles, the energy profile at nucleation time can in principle be calculated exactly by solving the inhomogeneous Klein-Gordon equation for the inflaton field with the appropriate tunneling-like initial conditions. The general structure is a spherically symmetric underdensity, with a thin wall, and a size of the order of H^{-1} (Coleman 1977). The internal matter content depends on the detailed shape of the transition potential. However, its successive evolution depends crucially on the properties of the dominating cosmic fluid. From Vadas (1993) we know that super-horizon voids, during the radiation dominated era (RDE), undergo hydrodynamical inflow of the primordial plasma into the empty central region. For an estimate of this effect we call η the mean velocity dispersion of the primordial plasma in units $c = 1$, where the cases $\eta = 0, 1$ mean respectively predominance and absence of CDM; simply, we sketch the filling process as inflow of cosmic fluid in a spherical empty void of comoving size $R/4$ (the 4 factor accounting for the overcomoving expansion) from the end of inflation

($T_e \simeq 10^{15}$GeV) across equivalence ($T_{EQ} \simeq 10$eV) until decoupling ($T_D \simeq 2 \cdot 10^{-1}$eV); one finds that the quantity Δ defined in (3) is given by

$$\Delta(t_D) = 1 - \exp\left[-\eta \frac{2H_o^{-1}}{R/4}\sqrt{\frac{T_o}{T_D}}\left(3 - \sqrt{\frac{T_D}{T_{EQ}}}\right)\right] \quad . (4)$$

For $R \simeq 10\ h^{-1}$Mpc our estimate gives $\Delta \simeq 1$ for $\eta = O(\frac{1}{100})$, a very typical value for CDM (La 1991). Thus, voids smaller than $R \simeq 10\ h^{-1}$Mpc are erased by matter inflow; this is therefore a lower cut-off in the distribution (1). We can see that larger voids ($R \simeq 10 \div 50\ h^{-1}$Mpc) have a typical filling fraction $.5 \geq \Delta \geq .1$ in their central underdense region. Since no significative dependence of our results upon these values exists, in the following we will assume $\Delta \simeq 0.3$.

We use exact metric models, built by Occhionero et al. (1981,1983), for the description of spherical, compensated structures directly in the matter dominated era (MDE). We investigate the metric distortion induced on the CMB radiation by the voids and check our approach by comparison with previous analyses of strongly non-linear highly approximated voids completely crossed by photons (Thompson & Vishniac 1987, hereafter TV). CMB complete crossing of voids was treated recently by some authors (Panek 1992, Arnau et al. 1993). We find that the metric CMB distortion in the case of complete crossing, Rees-Sciama effect (1968, hereafter RS), is negligible with respect to partial crossing, Sachs-Wolfe effect (1967, hereafter SW), for voids intersecting the last scattering surface (LSS), the width of which is modelled by making use of exact decoupling physics. Therefore, for treating accurately this case, we evaluate the CMB adiabatic distortion before decoupling due to the void. This is achieved by adapting the formalism developed by Hu and Sugiyama (1995, hereafter HS) to our case: it is shown that on scales in which SW effect is already comparable with the detected CMB anisotropies, the adiabatic effect is significatively reduced by Silk damping and then may be neglected. These results have been obtained by recovering, both for the SW and the adiabatic case, the angular dependence of the CMB temperature, which is therefore a function of the void size, of its exact density profile and of the particular position of the void with respect to the LSS; our model responds to all these items.

We anticipate that the largest void on the LSS that does not violate the COBE observations has a comoving size of $\simeq 25\ h^{-1}$Mpc , i.e. physical size 100 h^{-1}Mpc by today due to over comoving growth.

The content of this paper is as follows. In Sec.II we construct null geodesics . In Sec.III we analyse the CMB distortion induced by complete crossing of a void, comparing with previous results based on highly approximated models. Finally, in Sec.IV we consider the observational consequences of the voids lying on LSS. In the last section we draw the conclusions.

2 GEODESICS

The most natural theoretical enviroment to describe non-linear spherical large-scale perturbations was found by Tolman in 1934. We make the minimal assumption of pressureless fluid, according to the CDM paradigm.

The fundamental length element is ($c = 1$)

$$\begin{aligned} ds^2 &= dt^2 - \frac{1}{\Gamma^2(M)}\left(\frac{\partial r}{\partial M}\right)^2 dM^2 - \\ &- r^2(M,t)(\sin^2\theta d\phi^2 + d\theta^2) \quad , \end{aligned} \quad (5)$$

where M, the gravitating mass, plays the role of a radial coordinate, and $\Gamma(M)$, a generalization of the Lorentz γ, is a conserved quantity in the pressureless case; it is given by

$$\Gamma^2(M) = 1 + \left(\frac{\partial r}{\partial t}\right)^2 - \frac{2GM}{r} \quad . \quad (6)$$

Also

$$\rho(M,t) = \frac{1}{4\pi r^2 \partial r/\partial M} \quad . \quad (7)$$

The $\Gamma(M)$ function characterizes the perturbation structure. The choice $\Gamma = 1$ reproduces the unperturbed Friedmannian case. For hyperbolic perturbations, we write

$$\Gamma^2(M) = 1 + \Gamma_+^2(M)\,, \quad (8)$$

and the solution to Eq. (6) takes the form

$$r(M,t) = \frac{GM}{\Gamma_+^2(M)}(\cosh\eta - 1) \quad (9)$$

$$t = \frac{GM}{\Gamma_+^3(M)}(\sinh\eta - \eta) \quad . \quad (10)$$

The model that we use here for $\Gamma_+^2(M)$, Occhionero et al. (1981,1983), is suitable for description of a wide class of compensated matter structures, and has the following analytical form:

$$\Gamma_+^2(x) = B\left(\frac{L_s}{L}\right) x^{2/3}\gamma_n(x) \quad , \quad x = \frac{M}{M_*} \quad , \tag{11}$$

$$L_s = 2GM_* \quad , \quad L = \left(\frac{3M_*}{4\pi\rho_{\infty,o}}\right)^{1/3} \quad , \tag{12}$$

$$\begin{aligned}\gamma_n(x) &= \exp\left[-\left(\Gamma_E(1/n)/n\right)^n x^{5n/3}\right] \\ (\Gamma_E &\equiv \text{ Euler Function}).\end{aligned} \tag{13}$$

The model contains a tunable scale M_* that will be typically $10^{15}\mathrm{M}_0$ for a large scale void. The BL_s/L factor is a measure of the perturbation strength. The exponential in Eq.(13) sets to zero the perturbation for $M \gg M_*$; $\gamma_n(x)$ becomes a sharper and sharper stepwise function by increasing n, while simultaneously the compensating shell becomes narrower and denser; the coefficient in the exponent is dictated by the request of measuring the energy associated with the perturbation. With this model for $\Gamma_+(M)$, the dynamics is obtained solving Eqs.(9),(10).

We have now a model of spacetime; the next step is to integrate the null geodesics. We place the observer on the direction $\phi = 0$, $\theta = \pi/2$ from the void's center. A point on a null geodesic is marked by an affine parameter l, and the wave vector is

$$\left(K^t, K^M, K^\theta = 0, K^\phi\right) = \frac{d}{dl}\left(t, M, \theta = \frac{\pi}{2}, \phi\right) \quad . \tag{14}$$

The geodesic equations are

$$\frac{dK^t}{dl} = -\frac{1}{\Gamma^2}\frac{\partial r}{\partial M}\frac{\partial^2 r}{\partial t \partial M}\left(K^M\right)^2 - r\frac{\partial r}{\partial t}\left(K^\phi\right)^2 \quad , \tag{15}$$

$$\begin{aligned}\frac{dK^M}{dl} &= \left(\frac{\partial r}{\partial M}\right)^{-1} r\Gamma^2\left(K^\phi\right)^2 - \frac{1}{\Gamma}\frac{\partial \Gamma}{\partial M}\left(K^M\right)^2 - \\ &- 2\left(\frac{\partial r}{\partial M}\right)^{-1}\frac{\partial^2 r}{\partial t \partial M}K^t K^M - \\ &- \left(\frac{\partial r}{\partial M}\right)^{-1}\frac{\partial^2 r}{\partial M^2}\left(K^M\right)^2 \quad ,\end{aligned} \tag{16}$$

$$\frac{dK^\phi}{dl} = \frac{-2K^\phi}{r}\left(\frac{\partial r}{\partial M}K^M + \frac{\partial r}{\partial t}K^t\right) \quad . \tag{17}$$

Of these, Eq.(17) integrates directly into

$$K^\phi = \frac{k}{r^2} \quad , \tag{18}$$

where the constant k is fixed by the initial conditions. We now integrate numerically Eqs.(15)(16) and (18) using the normalzation

$$K^\alpha K_\alpha = 0 \quad , \tag{19}$$

as a check for the numerical accuracy. We set the "initial" conditions at the observation point P_0 and we integrate backwards. After choosing $(K^t)_0 = -1$, Eq. (19) at P_0 reads

$$\begin{aligned}(K^M)_0 &= \left[-\Gamma\left(\frac{\partial r}{\partial M}\right)^{-1}\sqrt{(K^t)^2 - \frac{k^2}{r^2}}\right]_0 = \\ &= -\left(\frac{3M}{r}\right)_0 \cos\alpha \quad ,\end{aligned} \tag{20}$$

where in the last equality, obtained by imposing that the observation point lies in the Friedmann region, α is the angle that the geodesic under investigation forms at P_0 with the direction of the void's center:

$$k = r_0 \sin\alpha \quad . \tag{21}$$

With the relations $K^\phi = (1/r)_0 \sin\alpha$ and $K^\theta = 0$, the initial conditions are complete. A similar approach to the construction of null geodesics on spherical structures was used firstly by Panek in 1992.

Finally, we know (see e. g. Anile & Motta 1976) that the CMB temperature measured by the observer is related to its value seen at any point x along the geodesic specified by α through the relation

$$\frac{T_x}{T_0} = \frac{(K_\mu u^\mu)_0}{(K_\mu u^\mu)_x} \quad , \tag{22}$$

where u^μ is the four-velocity of detection instrument. In the most interesting situation of a void intersecting the LSS, a peculiar velocity field causing a Doppler contribution exists at emission due to acoustic oscillations of the photon-baryon plasma: this contribution, evaluated in Sec.(IV) together with the dominant or comparable adiabatic effect, is small with respect to SW one because of Silk damping.

3 VOIDS IN FRONT OF THE LSS

As we already observed, a void, whether compensated or not, shows an over-comoving growth in an ordinary flat Friedmannian background. Then, in a first approximation, a void can be schematically represented as a region of space in which the scale factor $a(t)$ grows faster than $t^{2/3}$; more precisely, Bertschinger (1983,1985) found $t^{4/5}$ for compensated voids in the highly non–linear, asymptotic regime; our structures, being mildly non-linear, approximatively obey this law. Such a dynamics generates a cooling (redshift) in the CMB temperature (in addition, of course, to the ordinary one due to the unperturbed cosmic expansion).

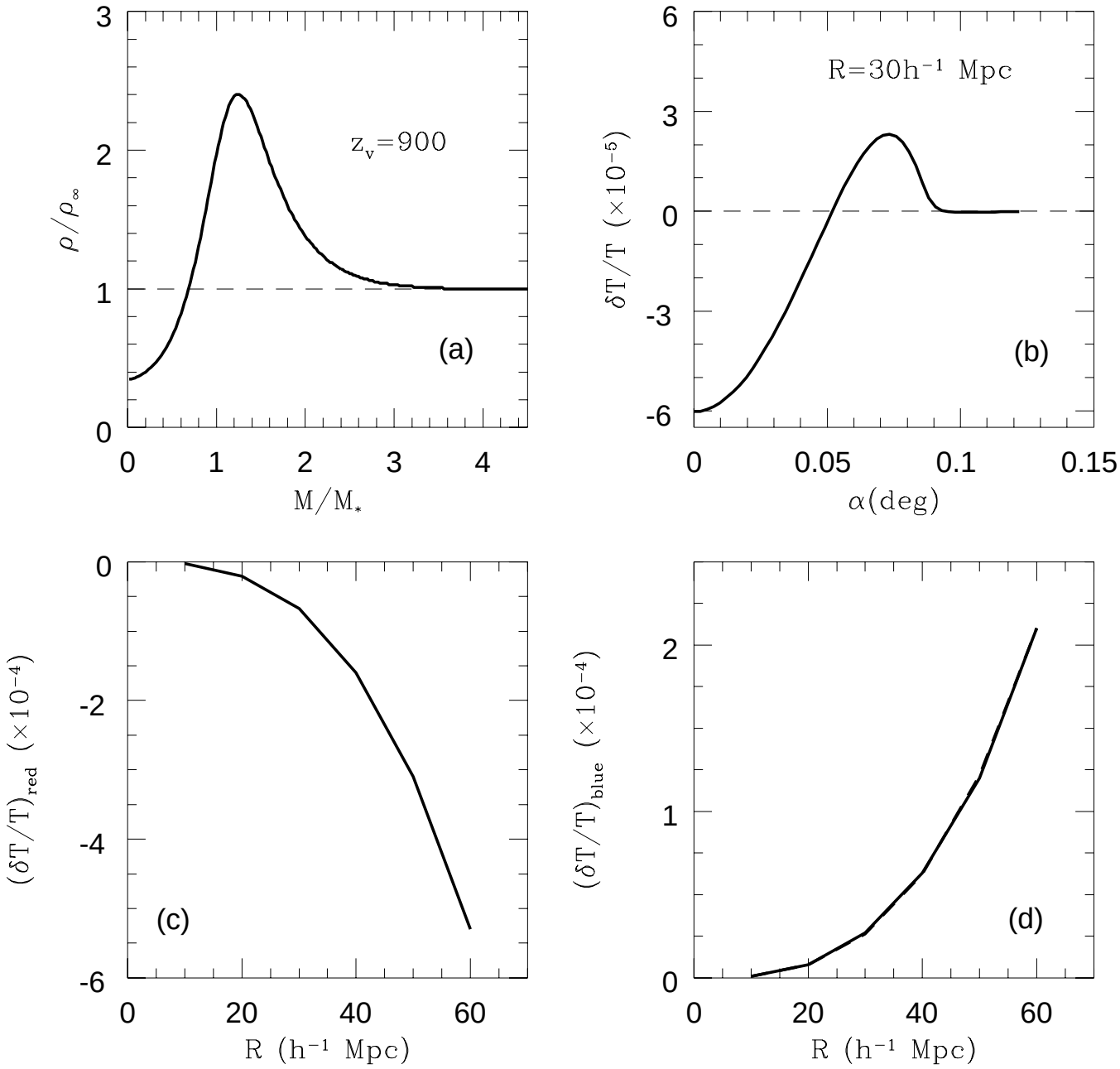

Figure 1. RS effect: void between us and the LSS; complete crossing of the void by the CMB photons. The non-linear density profile of panel *a* induces a very characteristic angular dependence on CMB temperature (panel *b*). In panels *c* and *d* dependence on R ($\sim R^3$) of the central redshift and of the peripheral blueshift.

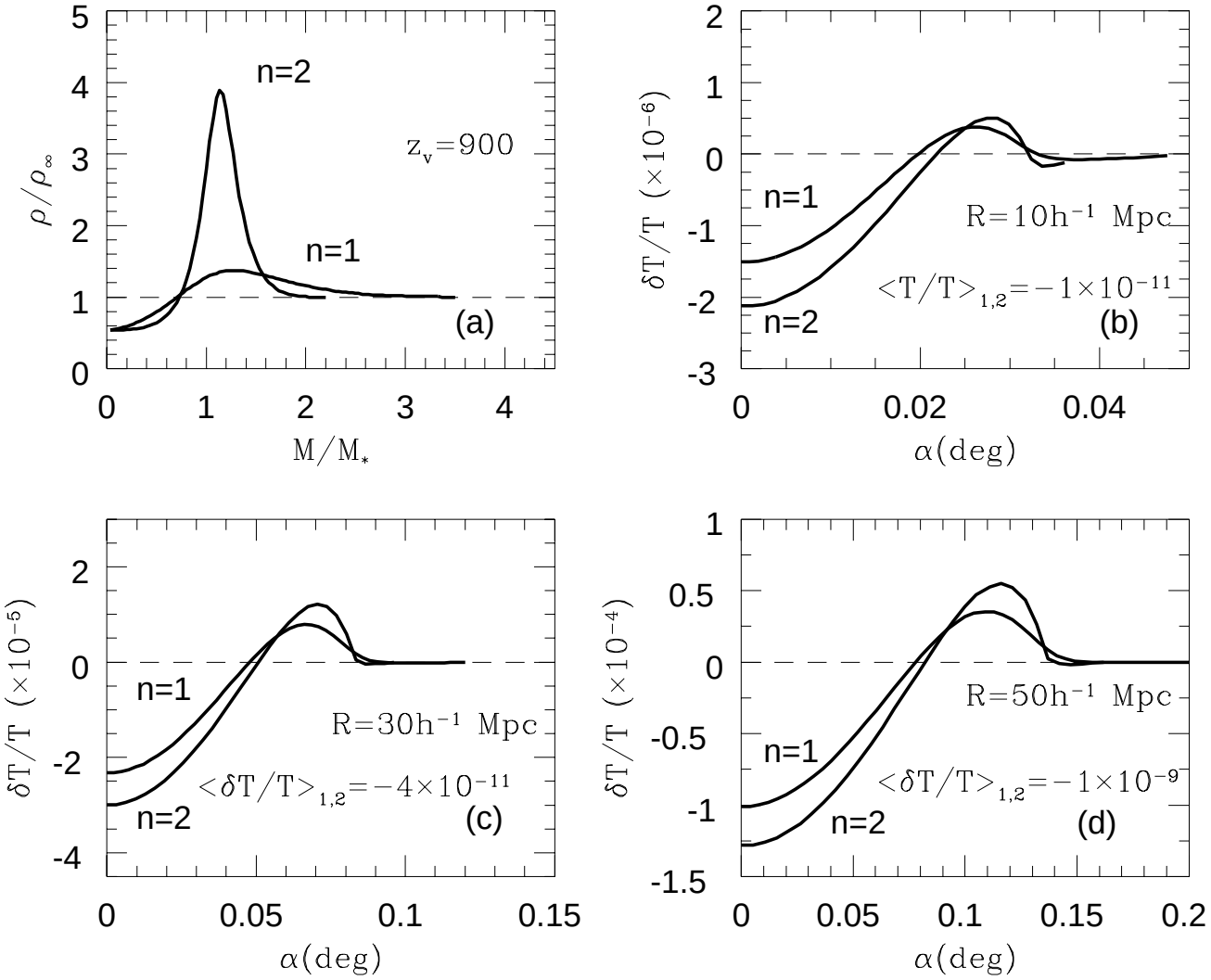

Figure 2. RS effect for different values of n (different sharpness of the density profiles) and for interesting values of the present radii. The values reported for $< \delta T/T >$, practically indistinguishable for n=1 and 2, are obtained by simulating COBE's angular resolution and appear much below the observed anisotropies.

On the other hand, the radiation is heated when crossing the void walls, as it is discussed below.

The case to be discussed here concerns a void at $z_v = 900$, completely crossed by a CMB photon. This case was analyzed in TV (firstly) and in recent works (Panek 1992, Arnau et al. 1993, Martinez-Gonzales et al. 1990). We leave to the next section the more important case of voids intersecting the LSS. TV found an analytical form for the angular dependence of the CMB temperature by adopting a model for the metric inside a compensated void which, albeit very schematic, contains all the essential aspects of the problem. As it is shown below, our result remarkably agrees with theirs. Their void is simply a spherical Friedmannian region of space in which the scale factor grows in time faster than in a $\Omega = 1$ universe, precisely as $t^{4/5}$. With an ingenious double Lorentz transformation, they find that photons entering and leaving the void are boosted by Doppler effect, simply because they are seen by frames moving towards them; on the contrary, during the void's crossing, they cool with respect to the flat Friedmannian case, because the space growth is faster. As the second effect is strongly dependent on the time spent by photons inside the void, while the first is almost fixed, the blueshift becomes dominant for strongly off axis trajectories.

Thompson & Vishniac's analytical result is:

$$\frac{\delta T}{T} = \left(\frac{R/(1+z)^{\cdot 2}}{H^{-1}}\right)^3 \cos\psi_\alpha \left(\frac{2}{5} - \frac{2}{3}\cos^2\psi_\alpha\right) \quad , \quad (23)$$

where ψ_α is the angle between the perpendicular to the shell and photon's direction at the leaving point; its expression as a function of α is

$$\psi_\alpha = \alpha + \\ + \cos^{-1}\left(\frac{d_v \sin^2\alpha}{R/(1+z)^{\cdot 2}} + \cos\alpha\sqrt{1 - \frac{d_v^2 \sin^2\alpha}{R^2/(1+z)^{\cdot 4}}}\right) \quad (24)$$

where d_v is the comoving distance of the void's center.

In Fig.(1) we report our numerical analysis of a typical void along the line-of-sight ($R = 30\ h^{-1}$Mpc , $z_v = 900$). Panel (a) shows the density profile as a function of the radial coordinate M normalized to M_*, the latter being calculated through the value ($\simeq R/4$) of the comoving radius at the time of interaction with the CMB. The central underdensity, obtained for $B = 2200$ in Eq.(11), and the large compensating shell are well visible. Panel (b) reports the CMB angular temperature change for complete crossing; the curve presents all the discussed features and agrees with the result of Eq. (23). A completely crossed void appears in the CMB sky as a cold circular spot sorrounded by a hot ring, because in off axis trajectories the hole contribution is suppressed. The value predicted by Eq. (23) for central trajectories is -10^{-4}; our result is slightly less because our voids are not completely empty. The maximal redshift to maximal blueshift ratio is -2.4 in Eq. (23) as in our case. Finally, note the smallness of angular sizes, due to the fact that this void is at the edge of the observed universe; the temperature distortion induced by such a structure is much below the experimental limit ($\simeq 10^{-5}$) because the present instrumentation has a finite angular width (3^o Gaussian beam for COBE). Panel (c) and (d) show the dependence of maximal redshift and blueshift on the void's radius. The solid line is numerical, while the dashed one, pratically indistinguishable from the first, is $(R/(1+z)^{\cdot 2}/H^{-1})^3$.

Now, let us come to the evaluation of the CMB dependence on the shell sharpness. As we stated above, the latter is regulated by the parameter n. We have confronted the CMB temperature changes induced by different n's, and for voids of different sizes in the interesting range. The results are shown in Fig.(2) and reveal a very weak dependence on n. The same happens during void crossing. In this case (the most interesting), for any value of the parameter BL_s/L in Eq. (11), large n makes γ_n in Eq.(13) approach the step function; in turn that yields the limiting sharpness for the shell's density profile. As we found that the variation of n does not change significatively the CMB perturbation (Eq. (35) below), we will neglect in the following this effect, and work with the simplest case $n = 1$. Also, Fig.(2) shows $< \delta T/T >$, defined as a COBE-like Gaussian-averaged signal:

$$< \frac{\delta T}{T} >= N \int \frac{\delta T}{T}(\alpha) \exp[-\alpha^2/2\gamma^2] 2\pi \sin\alpha d\alpha \quad , \quad (25)$$

where $\gamma = 3^o$, COBE's beam size, and N is the normalization constant; in the following, we will refer to the COBE Gaussian as $W(\alpha)$. It is evident that, as expected, the values reported in Fig.(2), of the order of 10^{-9} for the largest R, are extremely small compared with the observed anisotropies.

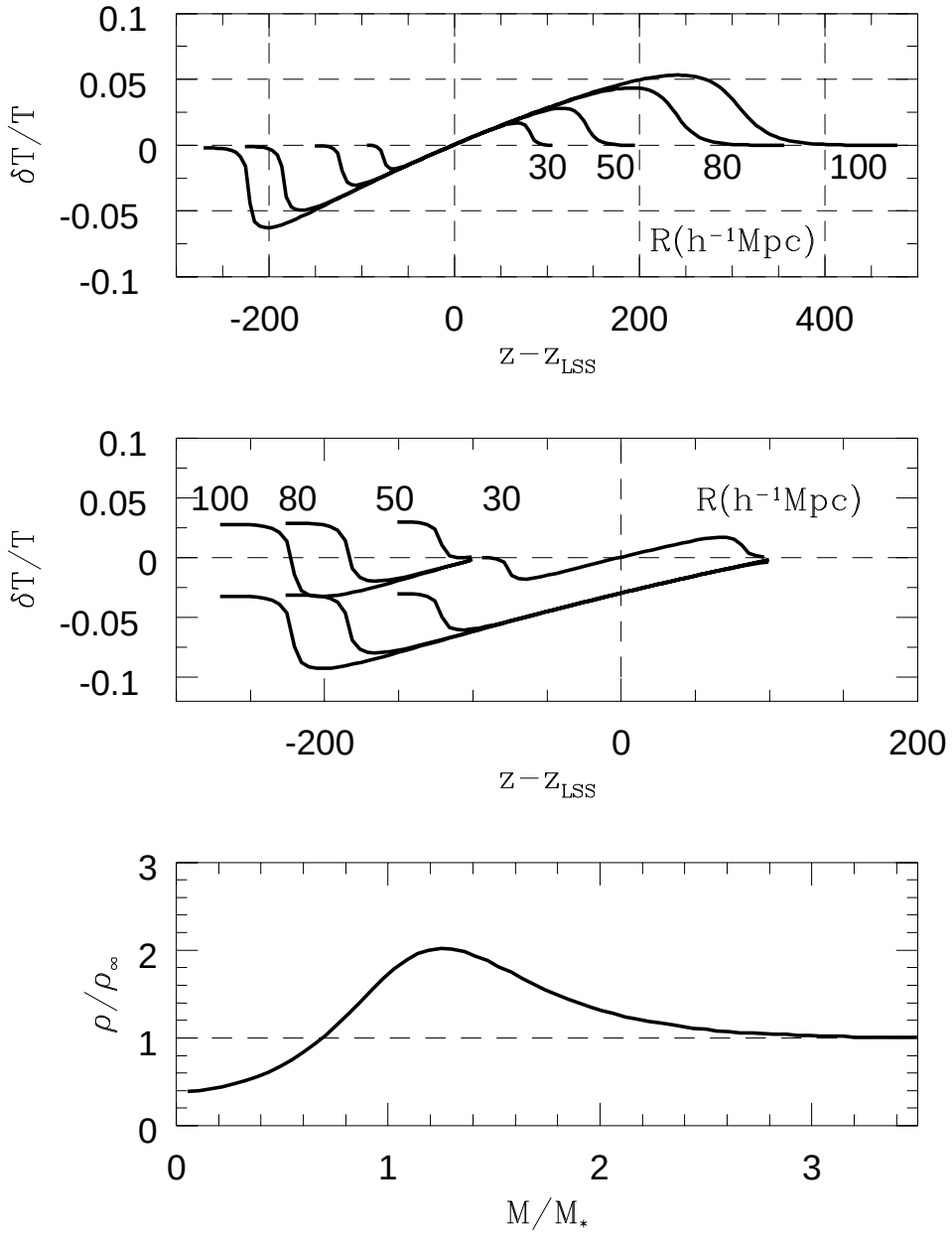

Figure 3. Temperature changes followed as functions of z along a central trajectory in voids with present physical radii R =30, 50, 80, 100 h^{-1}Mpc sitting exactly on the LSS. In panel a the photons come from infinity with vanishing $\delta T/T$; realistically, in panel b they leave either at $z = 1100$ or at $z = 900$; it is then seen that their frequency shift is either toward the red or toward the blue depending on the departing position. It must be remarked that the order of magnitude of this metric induced change is nearly 10^3 times its corrispondent value for complete crossing. Finally, panel c reports the underlying density profile.

We underline that this extreme smallness derives from the complete crossing of the void: in fact, the only observationally interesting voids are those intersecting the LSS, to be analyzed below. Furthermore, it must also be underlined that voids with $z \ll 1000$ will produce an even smaller temperature perturbation, because cosmic expansion, not compensated by the overcomoving growth, dilutes them.

4 VOIDS ON THE LSS

Fig.(3) shows the main new result of our work. In the upper and in the central panels we report the temporal evolution of the photon temperature during its crossing of the void: the latter is shown in the lower panel; different void radii of interest for the observations are shown. The abscissa is $z - z_{LSS}$, the latter being the redshift of LSS ($\simeq 1067$); in the four cases shown the void's center lies exactly on the LSS. In the upper panel the photons come from infinity with $\delta T/T = 0$ and experience firstly the blueshift from crossing the first shell, secondly the strong central redshift generated by the over comoving expansion, and finally the blueshift from crossing the second shell: globally this yields the small resulting $\delta T/T$ (RS effect) hidden on the left hand border of curves in Fig.(3). This is a very characteristic image of a void crossing, because we have found it being nearly the same in form for all the trajectories and astrophysically interesting void sizes. The central panel applies to realistic paths starting from either edge of the LSS ($z \approx 900$ and 1100) and displays the total blueshifts and redshifts that can be read on the left hand side. The order of magnitude of the temperature change during crossing is predicted by considering the propagation of a photon in a region of space expanding as $t^{4/5}$ during a time $\delta t \simeq R$; the result is

$$\left|\frac{\delta T}{T}\right| \simeq \frac{1}{5(1+z)^{\cdot 2}} \frac{R}{H^{-1}} \simeq \frac{1}{20} \frac{R}{H^{-1}} \quad , \tag{26}$$

where overcomoving growth is taken into account and H^{-1} is calculated at interaction epoch $z \simeq 1000$. As may be easily seen from the figure, the predicted value is strictly respected; this argument was inferred firstly by Vadas (1995). For the reason that $\delta T/T$ is proportional to the time spent in the void, for non-central trajectories R must be replaced with $R\sqrt{1-(\alpha/\alpha_R)^2}$, just the void's length on a direction characterized by the angle α defined in Sec.(II), the maximum value of which is α_R. An accurate analytic approximation of the results for all trajectories is

$$\frac{\delta T}{T} = \frac{R\sqrt{1-(\alpha/\alpha_R)^2}}{20\,H^{-1}}\, 1.25\, x \exp\left[-\left(\frac{x}{1.19}\right)^{10}\right] \quad , \tag{27}$$

where

$$x = \frac{r}{\sqrt{1-(\alpha/\alpha_R)^2}R/4} \tag{28}$$

and r is the photon's coordinate. We see that the sharpness is already very strong in the present case $n = 1$; increasing n up to infinity simply brings the curves in Fig.(3) to their limiting case

$$\frac{\delta T}{T} = \frac{R\sqrt{1-(\alpha/\alpha_R)^2}}{20\,H^{-1}}\, 1.25\, x\, \theta(|x|-1) \quad , \tag{29}$$

where θ is the Heaviside function. We also see that an axial trajectory presents a typical $\delta T/T$ *three orders of magnitude above* the central one of Fig.(1) (panel (b)), obtained for complete crossing and hidden on the left hand border of curves of the RS effect, displayed in the upper panel of Fig.(3). The reason why this strong contribution does not appear in Eq. (23) is that for complete crossing the effects of the shells and the central hole balance out, as it is evident from Fig.(3), leaving place to terms with higher power of R/H^{-1}. Therefore, if a void intersects the LSS, the ensuing $\delta T/T$ may be very different depending on the particular LSS position with respect to the center of the void. In any case, the amplitude will be much larger than in the case of complete crossing. Let us make a simple calculation: an useful approximation to the total temperature distortion induced by a void of angular size α_R averaged over a beam of size γ is

$$< \frac{\delta T}{T} > \simeq \left(\frac{\delta T}{T}\right)_{\alpha=0} \frac{\alpha_R^2}{\gamma^2} \quad , \tag{30}$$

and taking $\delta T/T|_{\alpha=0} \simeq 10^{-2}$ as a typical value from Fig.(3) we obtain for $R = 100\ h^{-1}$Mpc ($R = 25\ h^{-1}$Mpc at decoupling) and $\gamma = 3^o$

$$< \frac{\delta T}{T} > \simeq 6 \cdot 10^{-5} \quad . \tag{31}$$

This value, barely above the present observations, indicates that such scales are very close to the maximum permitted to primordial voids from CMB isotropy. This motivates the accurate investigation below.

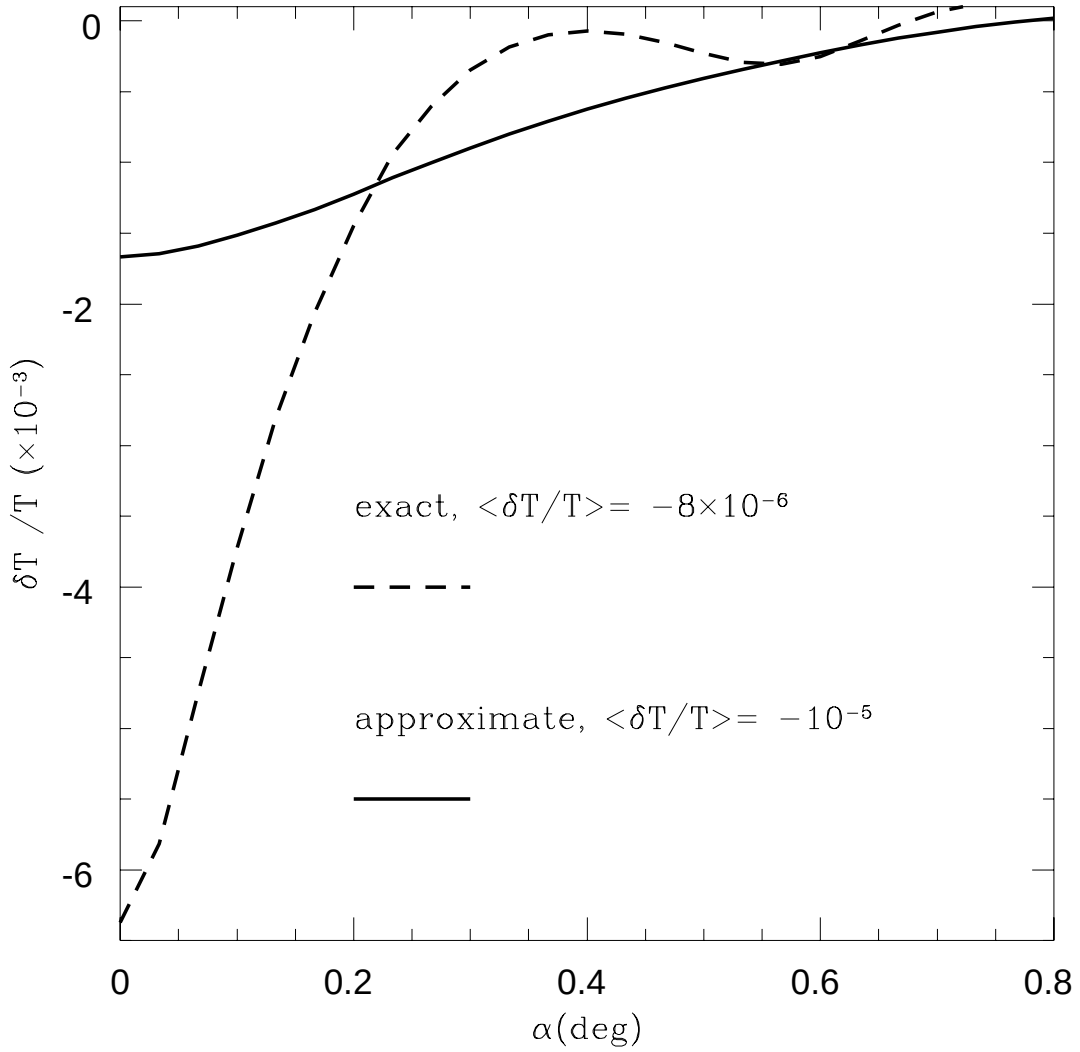

Figure 4. Purely adiabatic and Doppler $\delta T/T$ due to a compensated void in the cosmic fluid, both in the approximate (solid curve) and exact (dashed curve) case. On the relevant scales, this perturbation is well below the SW effect.

To treat accurately the case of voids intersecting the LSS, we must take care of all the physical processes at work. In fact the SW effect on the photons decoupled inside a void is not the only perturbation to the CMB; the corresponding inhomogeneity of the photon-baryon plasma naturally induces adiabatic and Doppler temperature fluctuations before decoupling. We anticipate that such contributions are reduced by Silk damping on scales $\leq 25\ h^{-1}$Mpc in which the SW effect is already comparable with the observed CMB anisotropy. To see this, we have used the formalism developed by HS; it allows to obtain the CMB fluctuations at decoupling caused by a perturbation characterized by a Newtonian potential ϕ (our perturbations are not properly in the linear regime, but this approximation allow us to estimate correctly the effect). In the HS treatment, the Boltzmann, Euler and continuity equations for the photon-baryon plasma, accounting for Thomson diffusion together with gravitational and pressure terms, are analytically solved under the tight-coupling approximation. In our treatment, in order to estimate only the adiabatic and Doppler effects, we have excluded the SW terms from HS formulas; we performed the calculus exactly and with the following simplifications: *a*) constant gravitational potentials, which is nearly true in the linear regime and approximatively in our mildly non-linear case; *b*) the quantity $3\rho_b/4\rho_\gamma$, that goes from 0 to .1 from the remote past to decoupling in models with $\Omega_b \simeq .01$, is neglected (equivalent to have a constant sound speed); *c*) istantaneous decoupling, and the Silk Damping scale taken at this time. With these hypotheses in the HS treatment, the amplitude of Fourier **k**-mode of temperature fluctuation at decoupling ($_D$) (we report only the monopole term for simplicity) is related to the potential by the simple and intuitive relation

$$\left(\frac{\delta T}{T}\right)_{k,D} = \phi_{k,D}\left(1-\frac{1}{2}\cos kc_s\eta_D\right)e^{-(k/k_D)^2} \quad , \quad (32)$$

where $\lambda_D = 2\pi/k_D = 3(\Omega_b h^2)^{-1/2})(\Omega_o h^2)^{-1/4}$ Mpc is the Silk damping scale at decoupling (again from HS formulas), and η is the conformal time. On scales larger than the sound horizon $c_s\eta_D$, Eq.(32) reproduces the known behaviour $\delta T/T \propto \phi$ up to a factor of the order of unity; on scales smaller than $1/k_D$ Silk damping forces to zero the inhomogeneities of the photon-baryon plasma. At intermediate scales, corresponding to $.2^o \div 1^o$ in the sky, an oscillatory behaviour occurs due to the acoustic oscillations; it will be retained in the form of Doppler peaks in the correlation function of $\delta T/T$. As in HS, one can antitransform $(\delta T/T)_k$ to obtain the contribution to $\delta T/T$ from the adiabatic effect as a function of the angle α. For the potential source we have used the simple model

$$\begin{aligned}
\frac{\delta\rho}{\rho}(r) &= -\delta\,, \quad \frac{r}{R} \leq 1 \ , \\
\frac{\delta\rho}{\rho}(r) &= \frac{\delta}{(1+a)^3-1}\,, \quad 1 \leq \frac{r}{R} \leq 1+a\,, \\
\frac{\delta\rho}{\rho}(r) &= 0\,, \quad \frac{r}{R} \geq 1+a\,, \qquad (33)
\end{aligned}$$

i.e. a central cavity of depth $1-\delta$ surrounded by a compensating thin shell $\Delta R = a \cdot R$. The result, together with the exact calculus, is shown in Fig.(4) for the interesting values $(1+z_D)\cdot^2 R = 25\ h^{-1}$Mpc, a=.5, $\delta = .7$ and the typical set $\Omega_b = .06, \Omega_0 = 1, h = .5$ for a CDM universe; the signal that COBE would detect for this perturbation is also reported and proves to be below the SW contribution, as we have anticipated.

Therefore, the picture of a primordial void sitting on the LSS which emerges very clearly from this analysis is that of a strong spot of metric origin and of either color on very small angular scales.

For the above arguments, we are also allowed to use the standard homogeneous model for the width of LSS. By taking into account the dependence of the fractional ionization on redshift z, and its consequences upon optical depth for photons, we are led to the probability function for a photon to be last scattered at redshift z (Jones and Wyse, 1985)

$$P(z) = \frac{5.26}{1000}\left(\frac{z}{1000}\right)^{13.25}\exp\left[-0.37\left(\frac{z}{1000}\right)^{14.25}\right] \quad (34)$$

that is well approximated by a Gaussian centered in $z_{max} \simeq 1067$ and with $\sigma \simeq 90$.

Now, let's use current observational data on the CMB isotropy to estabilish constraints on voids at decoupling. As we stated above, the qualitative form of the curves in Fig.(3) is the same regardless of the voids' radii. The COBE observed anisotropies distribution have an amplitude $\sigma \simeq 3 \cdot 10^{-5}$ at small angular scales (Bennett *et al.* 1994): therefore we will assume that a void is excluded by current observational data if its $< \delta T/T >$ is $3\sigma \simeq 10^{-4}$.

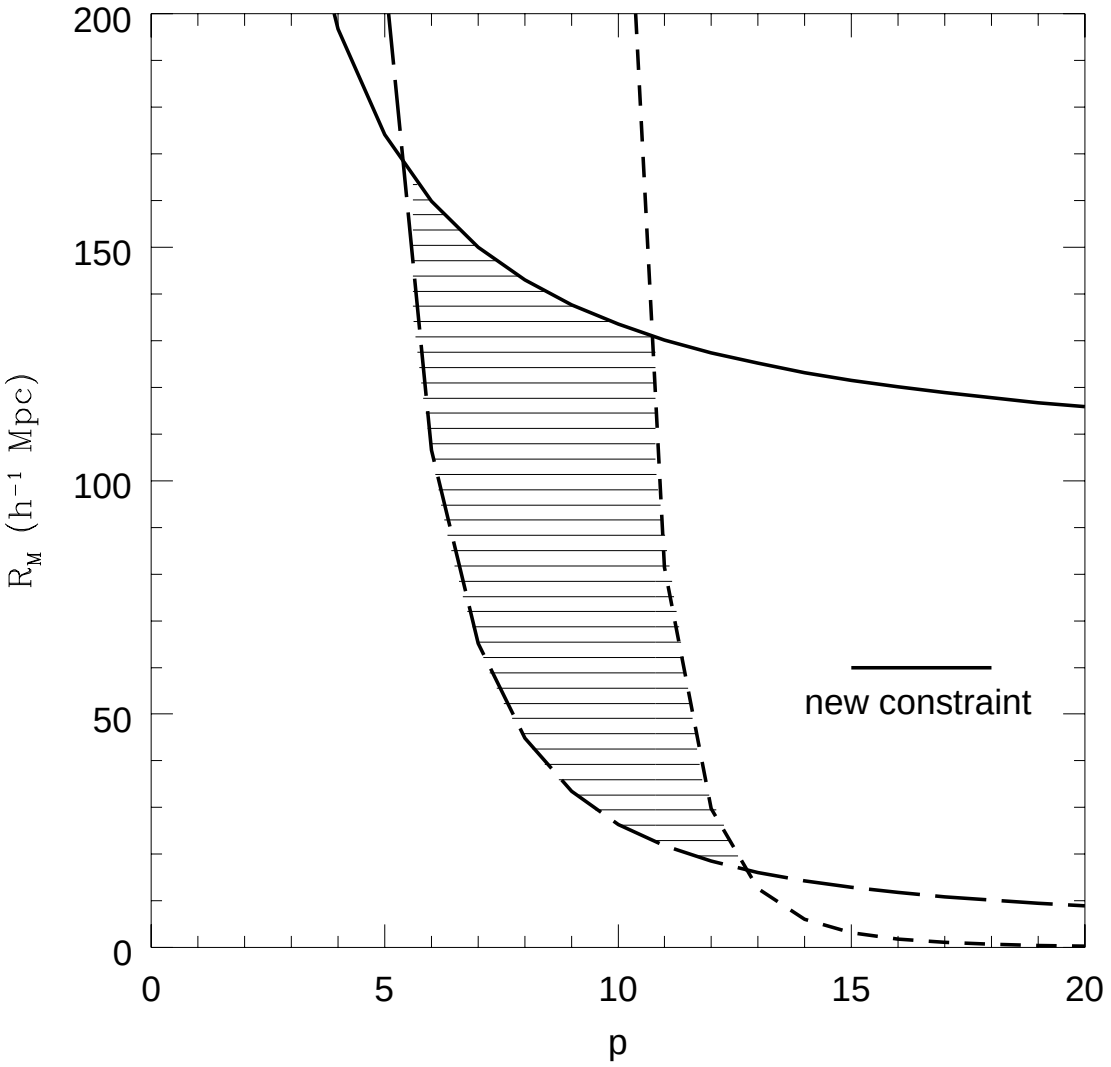

Figure 5. Observational constraints on the parameters p, R_M: the long-dashed line refers to the request that a reasonable fraction of space (50%) is filled by primordial voids; the short-dashed line is based on small hot spots statistics; the solid line is the present result: the number of voids inducing a visible CMB perturbation must be smaller than one. The shaded region gives the acceptable parameter space for primordial void distribution in the whole observed universe.

We have integrated the CMB fluctuation for many void radii in the relevant range, to get $< \delta T/T >$ as a function of R:

$$< \frac{\delta T}{T}(R) >= \int 2\pi \sin\alpha d\alpha dz \frac{\delta T}{T}(R,\alpha,z)\, W(\alpha) P(z)\ . \quad (35)$$

We can immediately obtain an upper limit for R as follows. At radial distance $(1+z)\cdot^2 r_{peak} = R$ inside the void, the CMB distortion, whether red or blue, reaches its maximal value before going to zero (see Fig.(3)). If r_{peak} coincides with the peak in $P(z)$ (at $z_{LSS} = 1067$), the CMB distortion detected by an instrument with Gaussian window function with width γ (expressed in degrees) is found to be

$$< \left|\frac{\delta T}{T}\right| > \simeq \frac{10^{-3}}{\gamma^2}\left(\frac{R}{H^{-1}}\right)^3 \quad , \quad (36)$$

where the numerical factor contains a correction 1/3 due to the LSS width for R near to H^{-1}. An R comes from the SW effect, while the remaining R^2 is due to the beam's angular width. Then, COBE-like experiments ($\gamma = 3^o$) say that no voids with $R = .97\, H^{-1} \simeq 100\ h^{-1}$Mpc (25 at decoupling) or more exist on the LSS. We point out that the same result without considering the LSS width would be $R = .63\, H^{-1}$.

Now that we have the largest void passing the CMB bounds, we pass to evaluate the statistical consequences on distribution (1). The position of the LSS peak with respect to the void center corresponds to a value of x defined in Eq.(28); for any x, there will be a radius $R_{max}(x)$ for which the CMB distortion detected by COBE would be nearly 3σ; this is obtained numerically from Eq.(35), putting the LSS peak at $r = x\, R$ from the void's center. The number of voids with comoving radius R is $|dN_B/dR|dR$, and the fraction of them having the LSS peak at distance between r and $r + dr$ is

$$dN(R,x) = \left|\frac{dN_B}{dR}\right| dR \frac{3\, dr}{2H_o^{-1}} = \left|\frac{dN_B}{dR}\right|\ R\, dR \frac{3\, dx}{2H_o^{-1}}\ . \quad (37)$$

The total number of such voids with $R \geq R_{max}$ must be less than 1; this is equivalent to the condition

$$\int_{-\infty}^{+\infty} dx \int_{R_{max}(x)}^{+\infty} dR \left|\frac{dN_B}{dR}\right| \frac{3\, R}{2H_o^{-1}} < 1 \quad . \quad (38)$$

By using Eq.(1) we obtain the following upper limit relation between R_M and p:

$$R_M < \left(\frac{p}{p-1}\int_{-\infty}^{+\infty} R_{max}(x)^{1-p} \frac{3\, dx}{2H_o^{-1}}\right)^{-1/p} \quad . \quad (39)$$

The result is shown in Fig.(5) as a solid line; values above the long-dashed line ensures that at least half of the space is presently filled by large scale voids ($R \geq 10\ h^{-1}$Mpc); values below the short-dashed line ensure that the random noise produced by an overposition of the many small voids on the CMB does not break the CMB isotropy (Amendola & Occhionero 1993). The dashed area contains roughly the set of (p, R_M) values

$$6 \leq p \leq 13 \quad , \quad 30\ h^{-1}\text{Mpc} \ \leq \text{R}_\text{M} \leq 130\ h^{-1}\text{Mpc} \quad , (40)$$

that is the parameter space for which the voids respect all the CMB constraints worked out so far, and provide large scale power matching current observations of galaxy clustering.

5 CONCLUSIONS

We have built a formalism that allows us to check the plausibility of the cosmogonic role of primordial voids; here, strictly speaking, by "primordial" we mean "present already at decoupling": however the obvious suggestion is that the voids originate much earlier, precisely in an inflationary first order phase transition. The constraints from the observations lie entirely in the compatibility of the voids' theoretical imprints on the CMB with the observed anisotropies at the relevant scales and translate into defining an allowed region of the parameter space for the void distribution.

In order to compute photon trajectories and temperature perturbations, we describe a void by an appropriate analytic general relativistic model of a spherical perturbation embedded in a flat Friedmann background.

Firstly we remind from the literature the case of a void lying between us and the last scattering surface (LSS): this implies the complete photon crossing known as Rees-Sciama effect. It is known that this induces a $\delta T/T \simeq -(4/15)(R/(1+z)\cdot^2 H^{-1})^3$: we have found that this results from a partial cancelation of the redshift occurring during the void crossing, namely the Sachs-Wolfe effect, with the blueshifts occurring at either shell crossing. Each of these effects, $|\delta T/T| \simeq R/20H^{-1}$, is three orders of magnitude larger than the total effect.

In the present paper, we have therefore considered the case of voids lying on the LSS and we have evaluated the global effect for photons decoupled inside

the void, comprising the Sachs-Wolfe contribution mentioned above, the adiabatic and Doppler effects due to the acoustical oscillations of the photon-baryon plasma; the latter has been found small with respect to the former because Silk damping is active on the small scales involved. For completeness, we have used an exact model for the LSS profile. Therefore, we are led to a very clear picture for the CMB impact of primordial voids: they are strong spots of metrical origin on very small angular scale.

A first observational constraint is obtained by requiring that the number of astrophysically interesting voids intersecting the LSS and capable of generating a distortion above the present observational limits on small angular scales, is smaller than unity. In practice this yields the available region of the parameter space for the void distribution, which we choose in the convenient form of a power law.

Where do we go from here? We expect a lot of power on the very small angular scales, $\ell \simeq 1000$ in the canonical expansion in Legendre polynomials of the CMB correlation function. Power on larger scales, $\ell \leq 100$, comes from the ordinary zero point fluctuations of the inflaton as well as from the variation of the number of voids in different regions of the sky, while in our case an unexpected strong correlation of metric origin arises on scales where Silk damping erases everything else. We plan therefore to build realistic sky maps by taking into account all the voids on the LSS in order to recognize whether the imprint of primordial voids will be actually present in the data of future high resolution experiments like $COBRAS - SAMBA$.

We thank David Wands and Michael Sahzin for useful comments.

REFERENCES

Abbott L. & Wise M. 1984 *Nucl.Phys* **B244** 541

Adams F. C. & Freese K. 1991 *Phys.Rev.* D**43** no.2, 353

Amendola L. & Borgani S. 1994 *Mon. Not. R. Astron. Soc.*

Amendola L. & Occhionero F. 1993 *Ap.J.* **413**, 39

Anile A. M. & Motta S. 1976 *Ap.J.* **207**, 685

Arnau J. V., Fullana M. J., Monreal L. & Saez D. 1993 *Ap.J.* **402**, 359

Bennet C. L., Kogut A., Hinshaw G., Banday A. J., Wright E. L., Gorski K. M., Wilkinson D. T., Weiss R., Smoot G. F., Meyer S. S., Mather J. C., Lubin P., Loewenstein K., Lineweaver C., Keegstra P., Kaita E., Jackson P. D. & Cheng E. S. 1994 *Ap.J.* **436**, 423

Bertschinger E. 1983 *Ap.J.* **268**, 17

Bertschinger E. 1985 *Ap.J.Suppl.* **58**, 1

Broadhurst T. J., Ellis R. S., Koo D. C. & Szalay A.S. 1990 *Nature* **343**, 726

Coleman S.*Phys.Rev.* 1977 D**15**, 2929

Da Costa L.N., Freudling W., Wegner G., Giovanelli R., Haynes M., and Salzer J.J. 1996 *Ap.J.* **468**, L5

Dubinski J., da Costa L.N., Goldwirth D. S., Lecar M. & Piran T. 1993 *Ap.J.* **410**, 458

El-Ad H., Piran T. & da Costa L. N., 1996 *Ap.J.* **462**, L13

Guth A. H., 1981 *Phys.Rev.* D**23**, 347

Hu W. & Sugiyama N. 1995 *Ap.J.* **444**, 489

Jones B. J. T. & Wyse R. F. G. 1985 *Astron. & Astroph.* **149**, 144

Icke V. 1984 *MNRAS* **206**, 1p

Kauffmann G. & Fairall A. P. 1991 *Mon.Not.R.Astr.Soc.* **248**, 313

Kolb E.W. 1991 *Physica Scripta* **T36**, 199

La D. 1991 *Phys.Lett.* B**265**, 232

La D. & Steinhardt P. J. 1989 *Phys.Lett.* B**220**, 375

La D. & Steinhardt P. J. 1989 *Phys.Rev.Lett.* **62**, 376

Liddle A. R. & Wands D. 1991 *Mon.Not.R.Astr.Soc.* **253**, 637

Liddle A. R. & Wands D. 1992 *Phys.Lett.* B**276**, 18

Linde A. D. 1983 *Phis.lett.* B**129**, 177

Lindner U., Einasto J., Einasto M., Freudlung W., Fricke K., & Tago E. 1995 *Astron. & Astroph.* **301**, 329L

Martinez-Gonzales E., Sanz J. L., Silk J. 1990 *Ap.J.* **355**, L5

Occhionero F. & Amendola L. 1994 *Phys.Rev.* D**50**, 4846

Occhionero F., Santangelo P. & Vittorio N. 1983 *Astron. & Astroph.* **117**, 365

Occhionero F., Veccia-Scavalli L. & Vittorio N. 1981 *Astron. & Astroph.* **97**, 169

Panek M. 1992 *Ap.J.* **388**, 225

Rees M. J. & Sciama D. 1968 *Nature* **217**, 511

Sachs R. K. & Wolfe A. M. 1967 *Ap.J.* **147**, 73

Scott P. F., Saunders R., Pooley G., O'Sullivan C., Lasenby A. N., Jones M., Hobson M. P., Duffett-Smith P. J., Baker J. 1996 *Ap.J.* **461**, L1

Thompson K. L. & Vishniac E. T. 1987 *Ap.J.* **313**, 517

Tolman R. C. 1934 *Proc.Natl.Acad.Sci.* **20**, 169

Turner M. S., Weinberg E. J. & Widrow L. M. 1992 *Phys.Rev.* D**46**, 2384

Vadas S. L. 1993 *Phys.Rev.* D**48**, 4562

Vadas S. L. 1995 in Proc. *Seventeenth Texas Symposium*, H. Boringer *et al.* eds., p. 710, NYAS, New York, NY

Vogeley M. S., Geller M. J. & Hucra J. P. 1991 *Ap.J.* **382**, 54

White S.D.M. & Ostriker J.P. 1990 *Ap.J.* **349**, 22